



# Effects of particle size distribution on the refractory properties and corrosion mechanism of ultra-low cement castables

Y. Kutmen Kalpakli\*

Department of Chemical Engineering, Yildiz Technical University,  
Davutpasa Kampüsü, 34210 Esenler, Istanbul, Turkey

\* Corresponding author: E-mail address: kalpakli@yildiz.edu.tr

Received 05.08.2008; published in revised form 01.12.2008

## ABSTRACT

**Purpose:** This study examines the effects of distribution of particle size-dimensions on refractory properties of alumina based castable refractories in which calcium aluminate cement (Secar-71) is used in low proportions as the hydraulic binder, which affects negatively properties of a refractory at high temperatures owing to its CaO content.

**Design/methodology/approach:** In this study the effect of particle size distribution on refractory properties of ultra-low cement castables was investigated. Secar 71 cement was used as a binder. The composition of refractory castable which consist of various particle size distribution was determined according to Andreasen packing model, with distribution coefficient (q) of 0.21, 0.22, 0.23, 0.24, 0.25 and 0.26. A cold crushing strength (CCS) of 93 MPa, a porosity value of 16.4% and a bulk density value of 3.12 g/cm<sup>3</sup> were obtained via a distribution coefficient of 0.26.

**Findings:** The mechanism of slag penetration on ULC for steel ladle was examined and the penetration layer was chemically analysed. Effects of mechanical properties on the corrosion mechanism were discussed.

**Research limitations/implications:** Determination of effects of particle size distribution on the refractory properties and corrosion mechanism of ultra-low cement castables.

**Originality/value:** The effects of particle size distribution on the refractory properties and corrosion mechanism of ultra-low cement castables were investigated.

**Keywords:** Ultra-low cement castables (ULC); Particle size distribution; Rheology; Slag penetration

## PROPERTIES

### 1. Introduction

In the recent years, there has been an increasing demand for castable refractories that can be produced with less energy and equipment. Along with the decrease in the proportion of cement, which serves as the hydraulic binder in low and ultra-low-cement refractory concretes and thus, an according reduction in the amount of CaO in a mixture, thermomechanical properties have improved and therefore these have become the mostly preferred class among castable refractories. Low and ultra-low cement castables are mainly used in high temperature applications.

Strength of such a material is measured according to its performance during a service. Thus, the main objective is the formation of a low porosity structure through densification of the material during sintering [1]. However, anorthite and gehlenite that are viscous liquid phases are shaped at 1400°C in "Low Cement (LC)" castables which have a CaO proportion between 1<CaO<2.5, which result in an increase on porosity of the refractory structure and accordingly cause loss in strength. It is possible to avoid a loss in strength at high temperatures, using super fine chrome-oxide or super fine calcined alumina instead of microsilica that can be found in the structure. Nevertheless,

chrome-oxide is not considered suitable in terms of environmental issues in most countries. Refractories can be exhibited maximum service life at high temperatures by lessening the proportion of CaO in its composition. In “Ultra-Low Cement (ULC)” refractories which have a CaO proportion between  $0.2 < \%CaO < 1$ , there takes place a strong mullite reaction at about  $1300^{\circ}C$  through addition of reactive alumina along with micro silica to tabular alumina structure. The formation of mullite leads to the formation of liquid phase and this contributes to strength of refractory at high temperatures. CaO content of refractory has certain effects on the formation of mullite. Existing CaO prevents the formation of mullite; thus loss of strength in Low-Cement castables at about  $1400^{\circ}C$ . However, as the cement content decreases, less liquid is formed theoretically; but increasing of strength is only possible when microsilica content falls below %6 [2, 3]. Development of the formulation which will enable the production of low porosity refractory is possible to control of particle size distribution of mixture. Decrease in porosity results in an increase in strength. As a result, decrease in the proportion of water used has positive effects on the spalling of material due to evaporation of water within the composition during firing. Two main studies in particle packaging belong to Furnas and Andreasen. Andreasen’s study is based on the fact that particle packaging of permanent particle size distribution in which all particle dimensions are displayed.

On the other hand, Furnas’ study has constituted the basis for the packaging of particles with different dimensions [4, 5]. Therefore, low and ultra-low cement compositions have been achieved. In castable refractories in which cement serves as the binder, cement that reacts with water ensures that mortar be placed and hardened, constituting various hydrate phases. Hydration reactions composed of high number of stages have been studied widely [2, 6 and 7].

Monocalcium aluminate phase and  $CA_{12}A_7$  and  $CA_2$  phases which are the most significant phases in calcium aluminate cements and in which hydration reactions develop fairly rapidly are the phases which develop mechanical characters of cement while refractory is hardened. Particularly, existence of  $CA_{12}A_7$

has significant effects on rapid hardening of low cement castable refractories [8].

This study examines the effects of distribution of particle size-dimensions on refractory properties of alumina based castable refractories in which calcium aluminate cement (Secar-71) is used in low proportions as the hydraulic binder, which affects negatively properties of a refractory at high temperatures owing to its CaO content. In castable refractory composition, in addition to tabular alumina, super fines such as micro silica and reactive and calcined alumina which play significant roles in particle packaging, improvement of rheological properties of a material and increase in its performance in service temperature exist as well. Optimum particle size distribution was determined after experimental studies.

## 2. Experimental procedure

### 2.1. Raw materials

In this experimental work, tabular alumina which was supplied from Almatiss<sup>TM</sup> Company was used as refractory aggregate. Secar 71 calcium aluminates cement was used as a binder.

Furthermore  $Q_1$  quality micro silica was used which was supplied from RW silicium GmbH as a super fine material in the mixtures.

The chemical composition and physical properties of tabular alumina, Secar-71 Calcium aluminates cement and micro silica are given Tables 1 and 2.

The graphic of the particle size distributions of tabular alumina, reactive alumina, calcined alumina, micro silica and Secar 71 Calcium aluminates cement which were added into the mixture as super fines are displayed in Figure 1. Moreover the graphic of the particle size distributions of ADS1 and ADW1 which were added into the mixture as materials by using coordination of blend solidification point. This analysis results is also given in Figure 1. The particle size distribution analyses of these materials were done by using a Malvern<sup>TM</sup>, Mastersizer 2000 instrument.

Table 1.  
The chemical composition and physical properties of tabular alumina and Secar-71 Calcium aluminates cement

Raw Materials	Chemical Composition	(%)
	CaO	27
	$Al_2O_3$	72
Secar 71	$Na_2O$	Max:0.30
Calcium aluminates cement	$SiO_2$	Max:0.30
	$Fe_2O_3$	Max:0.20
	MgO	Max:0.40
	$Al_2O_3$	>99.4
	$Na_2O$	0.60
	$SiO_2$	$\leq 0.12$
	$Fe_2O_3$	$\leq 0.30$
Tabular alumina	Physical Properties	
	Bulk Specific gravity ( $g/cm^3$ )	$\geq 3.5$
	Apperant Porosity (%)	$\leq 5$
	Water Adsorption (%)	$\leq 1.5$

Table 2.

The chemical composition of Micro silica

Raw Materials	Chemical Composition	(%)
	SiO <sub>2</sub>	97.00
	SiC	0.50
	MgO	0.30
	Al <sub>2</sub> O <sub>3</sub>	0.15
Micro silica	CaO	0.20
	Na <sub>2</sub> O	0.05
	K <sub>2</sub> O	0.80
	Fe <sub>2</sub> O <sub>3</sub>	0.03

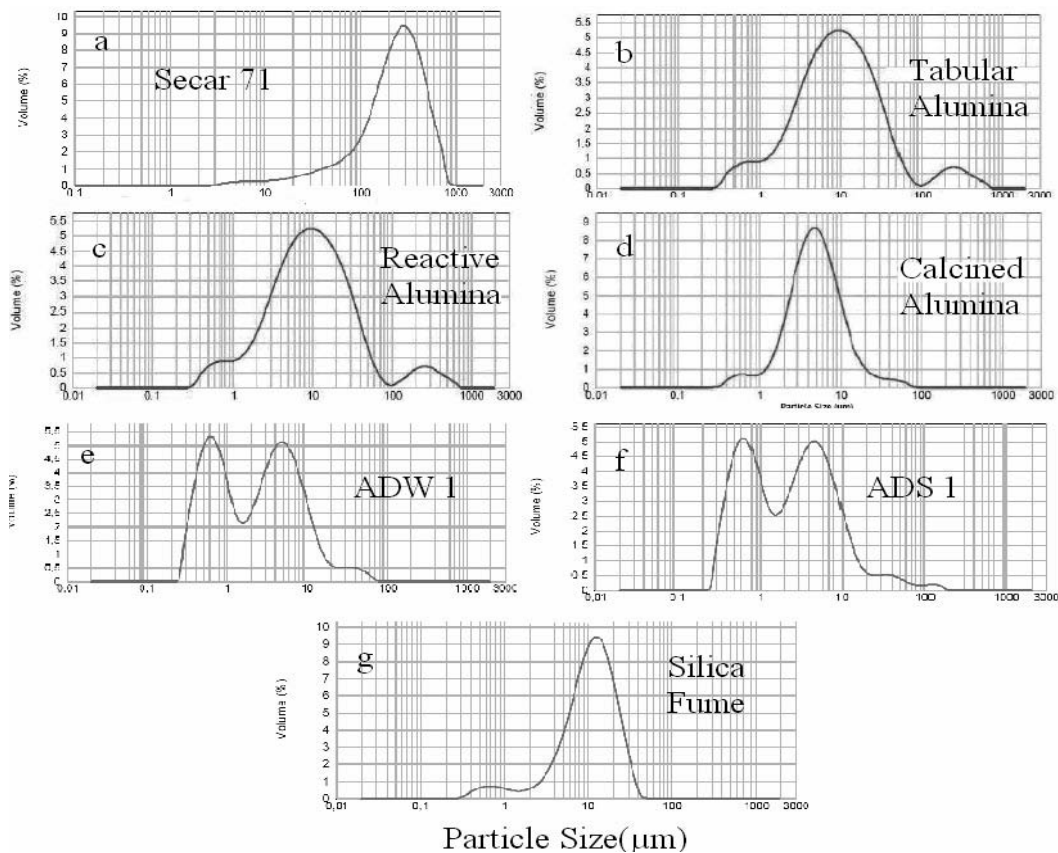


Fig. 1. Particle size distributions of a) secar 71, b) tabular alumina(-0.04 mm), c) reactive alumina, d) calcined alumina, e) ADW1, f) ADS1, g) Micro silica

## 2.2. Sample preparation

Prior to running experiments, tabular alumina was screened to the defined ranges of the particle size. Reactive alumina, calcined alumina, silica fume and calcium aluminates cement were added to the mixture as superfines ( $<0.04 \mu\text{m}$ ). The Andreassen equation was used to determine the ratios of the range of the particle size of the alumina according to the particle size distribution parameter( $q$ ) in this study. The  $q$ -values were varied as 0.21, 0.22, 0.23, 0.24, 0.25, 0.26 to define which one suit to the consumed

raw material were listed in Table 3. In all experiments, reactive alumina, calcined alumina, micro silica and calcium aluminates cement and organic fiber were added at constant amounts of 7 wt.%, 4 wt.%, 0.5 wt.%, 2.5 wt.% and 0.08 wt.% respectively. Each batch was firstly dry mixed in a Hobart™ A200 mixer for 2 minutes. Afterwards the pre-mixed slurry of blend is added respective water contents given in Figure 2 and wet mixing is carried out for about 5 minutes. The homogenized mixture was cast into molds of 5x5x5 cm onto a vibrating table with 50Hz vibrating rate. The sample were kept for 24 hrs at room

temperature for one day and then cured at a temperature of 110°C for 24 hrs in a Binder™ type incubator. The refractory samples were sintered at 1500°C for five hours in a Protherm™ high temperature chambers furnace at a heating rate of 10°C/min. After firing, porosity, bulk density, water absorption, cold crushing strength, slag test were carried out. Apparent porosity, bulk density, water absorption were measured by water immersion method according to DIN 51056 standard. The cold crushing strength tests of samples were done according to DIN 51067 standard. Cold crushing strength was measured by an Atom Teknik™ instrument.

### 3. Results and discussion

#### 3.1. Effect of particle size distribution parameter on the water consumption

During mixing, the addition of the ratio of the water is very important because it affects the final product considerably. When the particle size distribution parameter increases, the amount of coarse particles which used in the batch increases. Therefore the specific surface area of the particles decreases and less water was consumed because of this. The reduction of the amount of the consumed water as a function of increasing particle size distribution parameters is shown in Fig. 2.

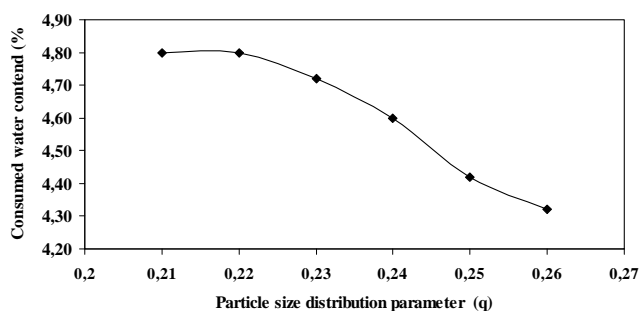


Fig. 2. Water content as a function of particle size distribution parameter

#### 3.2. Effect of particle size distribution parameter on the water adsorption, apparent porosity and bulk density

Bulk density and apparent porosity are important physical properties for the refractory industry. The porosity and bulk density variations of the samples as a function of particle size distribution parameter are indicated in Figs. 3, 4 and 5, respectively.

Table 3.

Weight percentages of the compositions of the samples according to q values which were used in the experiments

Tabular Alumina Particle Size Range(mm)	And.Mod. q = 0.21 (g)	And.Mod. q = 0.22 (g)	And.Mod. q = 0.23 (g)	And.Mod. q = 0.24 (g)	And.Mod. q = 0.25 (g)	And.Mod. q = 0.26 (g)
5 – 6.3	4.74	4.96	5.18	5.40	5.62	5.83
4 – 5	4.36	4.55	4.74	4.93	5.14	5.29
3.13 - 4	4.45	4.63	4.82	5.00	5.18	5.36
2 – 3.15	7.87	8.17	8.46	8.75	9.03	9.30
1 – 2	10.64	10.99	11.32	11.63	11.95	12.24
0.5 – 1	9.21	9.43	9.65	9.85	10.04	10.22
0.25 – 0.5	7.95	8.10	8.22	8.34	8.44	8.53
0.1 – 0.25	8.88	8.96	7.01	9.10	9.15	9.18
0.063 – 0.1	3.88	3.89	5.92	3.88	3.86	3.86
0.040 – 0.063	3.46	3.45	3.44	3.43	3.40	3.36
- 0.040 (pan)	34.56	32.87	31.24	29.69	28.19	26.83
Reactive alumina	7.00	7.00	7.00	7.00	7.00	7.00
Calcined alumina	4.00	4.00	4.00	4.00	4.00	4.00
Secar-71	2.50	2.50	2.50	2.50	2.50	2.50
Micro Silica	0.50	0.50	0.50	0.50	0.50	0.50
ADS1	0.50	0.50	0.50	0.50	0.50	0.50
ADW1	0.50	0.50	0.50	0.50	0.50	0.50
Organic fiber	0.08	0.08	0.08	0.08	0.08	0.08
Water	4.80	4.80	4.72	4.60	4.42	4.32

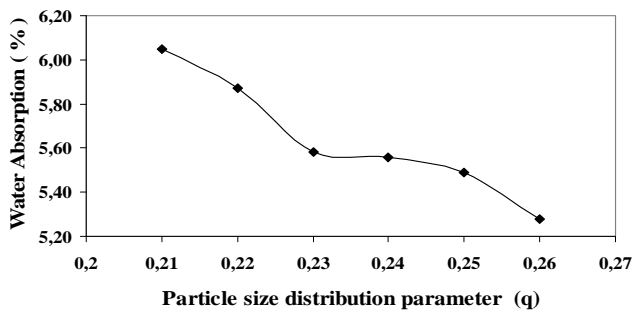


Fig. 3. Water absorption as a function of particle size distribution parameter

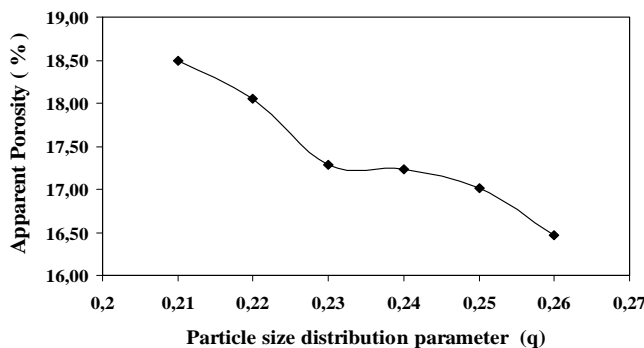


Fig. 4. Apparent porosity as a function of particle size distribution parameter

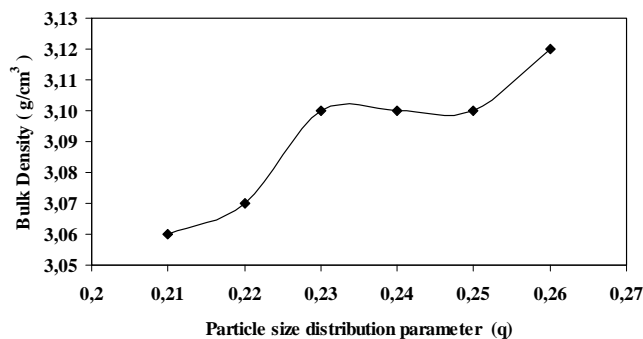


Fig. 5. Bulk density as a function of particle size distribution parameter

As seen in Fig.5 the sample which was produced according to  $q=0.26$ , has a higher bulk density and less apparent porosity when compared with the other samples. Since decreased amount of fine particles were used in this batch, vibration application capability increases and in this way particle packing and characteristics were improved. In other words the optimization of particle size distribution is provided that voids between the coarse particles are filled by the fine particles.

### 3.3. Effect of the particle size distribution parameter on the cold crushing strength

It is shown in Figure 6 that the cold crushing strength of the sintered samples at  $1500^{\circ}\text{C}$  increases with increasing particle size distribution parameter. The mixture which is prepared for  $q=0.26$  has the lowest fine and superfine particles. Thereby, vibration application capability of the blend is quite well. The fine and superfine particles fill into the voids in a castable between coarse particles for vibratory applications and the particle packing of the sample which is produced according to  $q=0.26$  is better than the others. Due to the fact that this sample has better mechanical properties in comparison to the others.

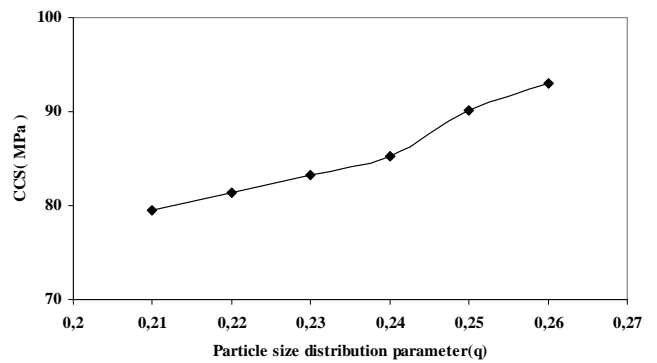


Fig. 6. Cold crushing strength as a function of particle size distribution parameter

### 3.4. Slag corrosion test (crucible method) for corroded castable by steel ladle slag

Ladle slag supplied from the Steel Plant of Erdemir Inc. has been utilized in order to be used in the corrosion tests of the castable samples. The chemical composition of this slag was given in Table 4. The slag which comprised mainly  $\text{CaO-Al}_2\text{O}_3\text{-SiO}_2$  and contained 17.66% iron in solution. It was granulated and sieved using a  $100\ \mu\text{m}$  sieve. The powdered slag under the sieve was separated in order to be used in the corrosion test.

Slag charge were applied to the inside of the castable crucible pot samples prepared according to DIN 51069 and were sintered at  $1600^{\circ}\text{C}$  for 4 hours in a Protherm<sup>TM</sup> high temperature chambers furnace at a heating rate of  $10^{\circ}\text{C}/\text{min}$ . Castable samples which interacted with the slag were cut as stated in DIN 51069 and their corrosion surfaces were examined.

An intense slag region comprising "dissolution" and "penetration" areas were observed in the interfaces. This corroded sample is shown in Figure 7a. Slag penetration areas was measured with the use of a semi-quantitative graph measurement paper. As shown in Figure 7b; slag penetration area is obtained  $426\ \text{mm}^2$ .

Table 4.  
Chemical composition of ladle slag (%) (C/S = 2.29)

	FeO/Fe <sub>2</sub> O <sub>3</sub>	SiO <sub>2</sub>	MnO	Al <sub>2</sub> O <sub>3</sub>	CaO	MgO	P <sub>2</sub> O <sub>5</sub>	S	Na <sub>2</sub> O	K <sub>2</sub> O	TiO <sub>2</sub>	Cr <sub>2</sub> O <sub>3</sub>
wt-%	17.66	14.32	4.62	14.02	32.87	7.01	0.617	0.221	0.001	0.107	0.483	0.114

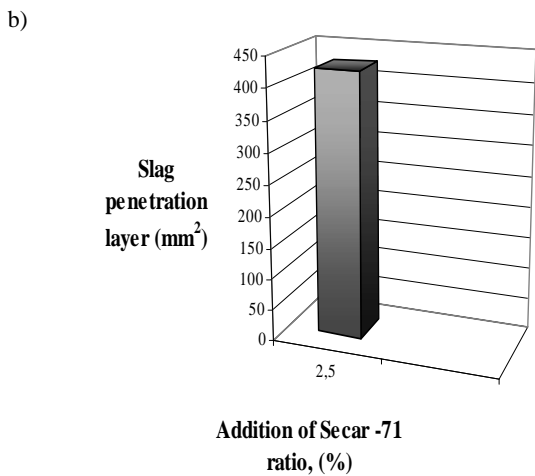
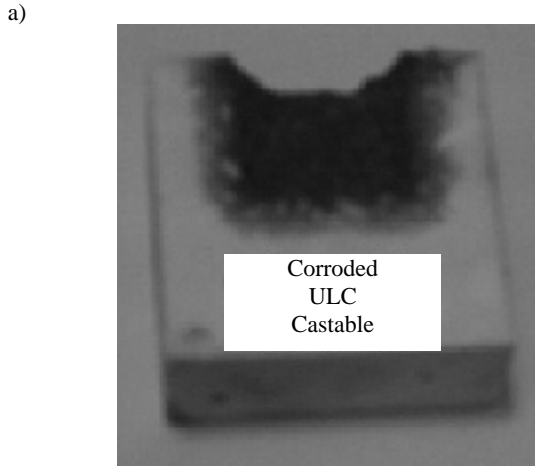


Fig. 7 a-b. Slag penetration areas images (a) and slag penetration areas of castable at 1600°C

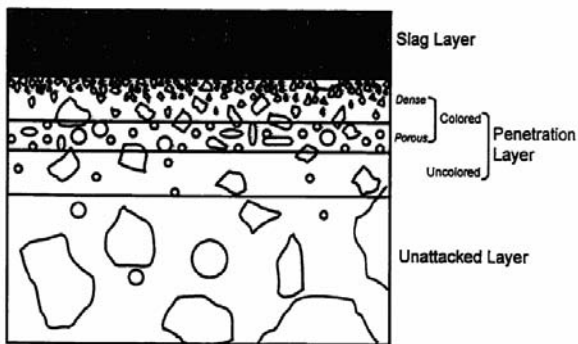


Fig. 8. Schematic diagram of general image of castable after slag corrosion

The microstructure characteristic of corroded castable by ladle slag is schematically illustrated in Fig. 8. It shows that three different layers section: slag layer, penetration layer and unattached refractory castable layer section are given in the diagram.

To examine the slag corrosion in detail, ULC castable corroded at 1600°C was investigated. Fig. 9. shows SEM image of the slag region.

As seen in the SEM photographs, hot zone depth is measured as <4mm in ULC castable.

Fig. 10 shows the lineScan analysis from the slag contact zone of the same region to the inner sections of castable.

Fig. 11 a-b-c shows the EDS point analysis extending from the slag contact zone of the same region to the inner sections of the refractory and gives the corresponding chemical composition of ULC castable. EDS results in the figure are taken from the corroded zone (hot zone), uncorroded refractory zone (cold zone) and border between the hot- and cold zone (border zone).

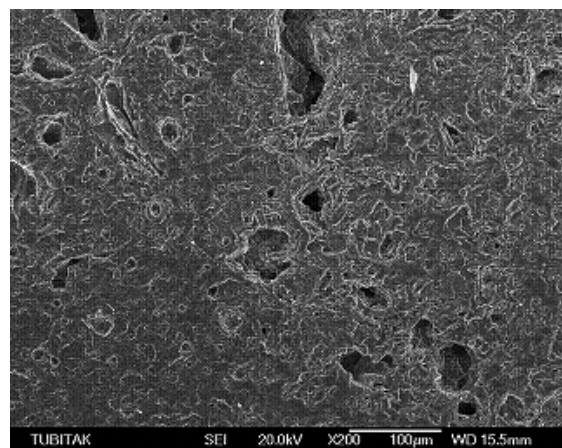
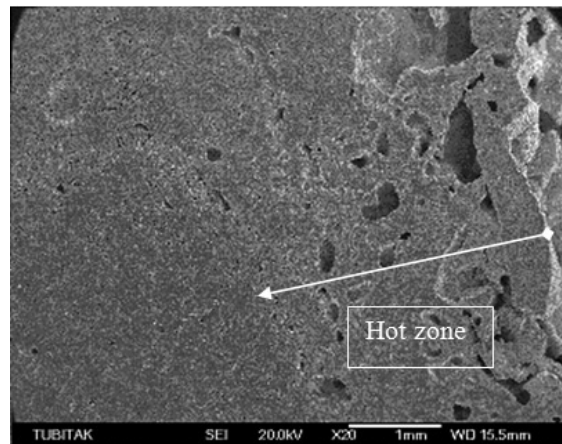


Fig. 9. TEM potomicrograph (20x) of the castable at hot zone

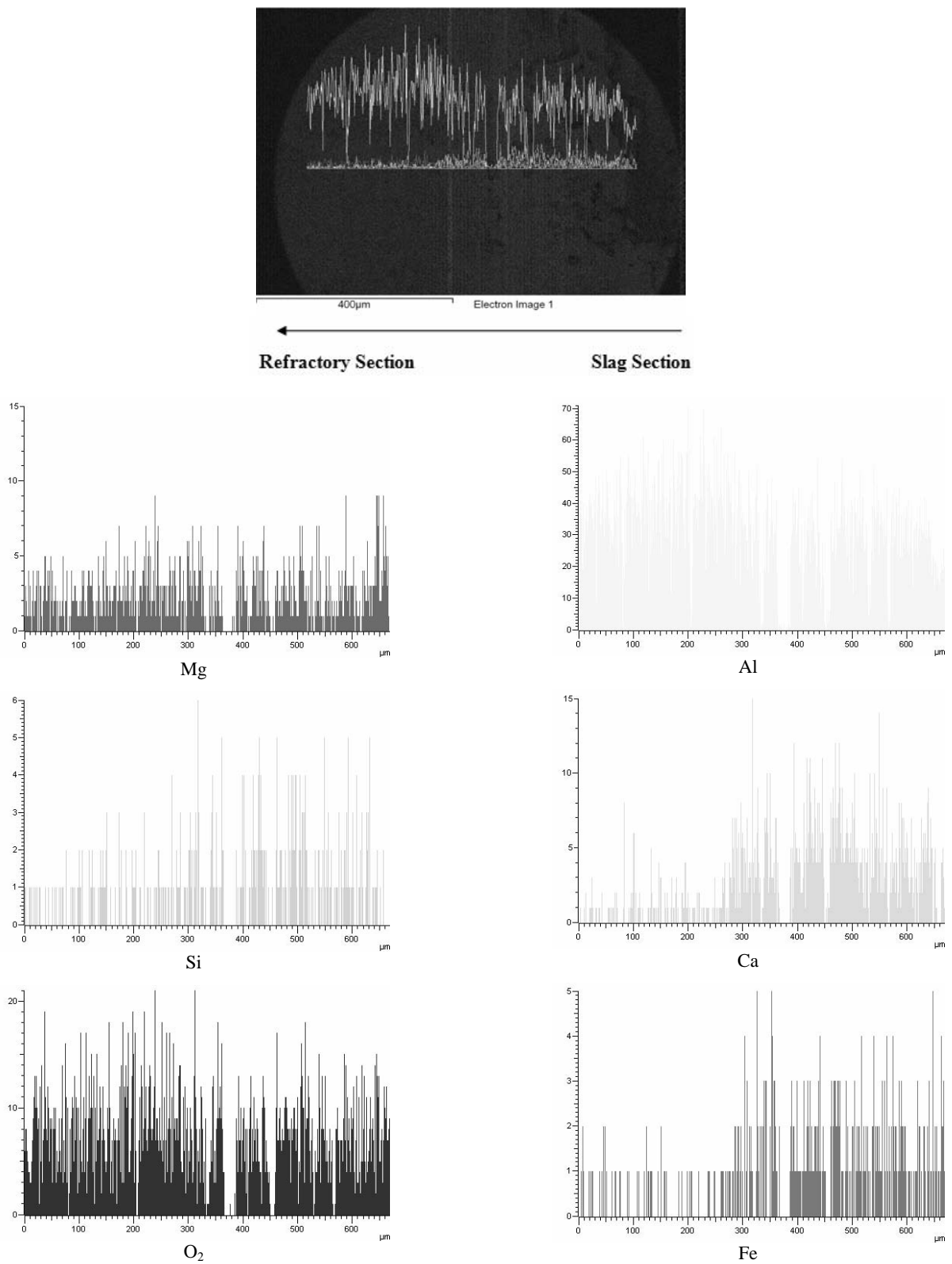
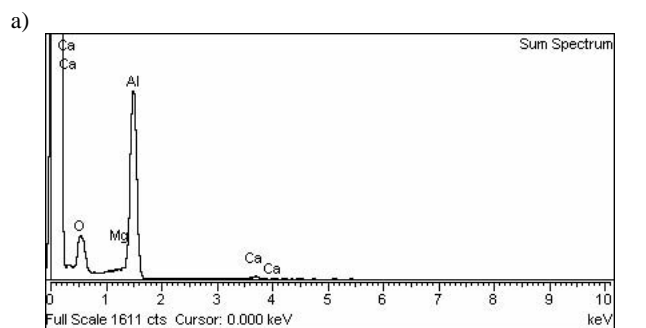
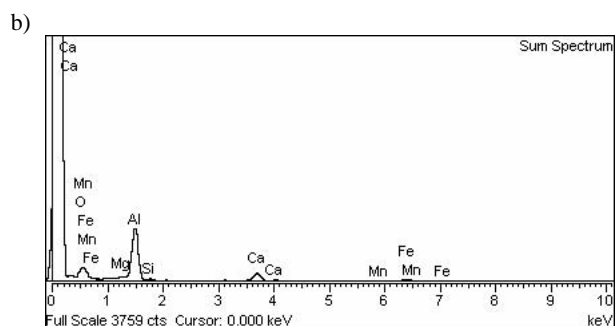


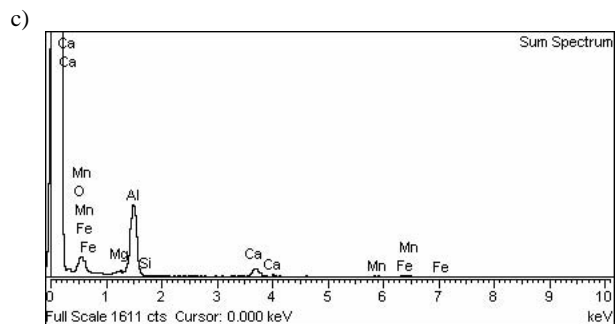
Fig. 10. LineScan analysis of slag penetration layer in castable



Element	Weight%	Atomic%
O K	36.14	49.02
Mg K	0.23	0.20
Al K	62.15	49.98
Ca K	1.48	0.80



Element	Weight%	Atomic%
O K	37.45	52.96
Mg K	0.83	0.77
Al K	44.09	36.97
Si K	1.28	1.03
Ca K	10.22	5.77
Mn K	1.00	0.41
Fe K	5.13	2.08



Element	Weight%	Atomic%
O K	40.97	56.38
Mg K	1.13	1.02
Al K	43.70	35.66
Si K	0.16	0.13
Ca K	8.21	4.51
Mn K	0.93	0.37
Fe K	4.89	1.93

Fig 11. EDS analysis of slag penetration layer in castable; a) cold zone, b) border zone, c) hot zone

Free  $\alpha$ - $\text{Al}_2\text{O}_3$  in castable composition and FeO,  $\text{Fe}_2\text{O}_3$  and MnO coming from slag have a low chemical interaction. Thus, it is seen in Figures 10 and 11 that Fe- and Mn- ions coming from slag are penetrated to samples in a very limited way.

On the other hand, as a result of the reaction of CaO,  $\text{SiO}_2$  found in castable composition and coming from slag with  $\alpha$ - $\text{Al}_2\text{O}_3$ , calcium-alumina-silicate phases that has a eutectic point at a low temperature like  $1170^\circ\text{C}$  began to be formed. When the components of gehlenite with melting point  $1590^\circ\text{C}$  and of anortite with  $1550^\circ\text{C}$  are formed, refractory undergoes an intensive corrosion till inside. When the results of EDS analysis given in Figure 10 are investigated, the fact that CaO were found out in hot and border zones at a high level shows that these phases might have been formulated.

## 4. Conclusions

Solidification point of castable was determined as 3 hours at  $25^\circ\text{C}$  room temperature. When the particle size distribution module was changed from 0.21 to 0.26; it was found out that refractory properties improved. In these refractories when the particle size distribution module was 0.26, Cold crushing strength of the material prepared with water of 4.32 % rate was 93 MPa, apparent porosity was 16.4% and bulk density was  $3.12 \text{ g/cm}^3$ .

## Acknowledgements

I would like to thank to Superateş Refractories Company for their support throughout this investigation.

## References

- [1] I.I. Nemets, V.V. Strokova, V. Zubashchenko, Kinetics of Sintering of a Low-Cement Corundum Castable Modified by an Eutectoid Phase, *Refractories and Industrial Ceramics* 45/3 (2004) 214-216.
- [2] S. Banerjee, *Monolithic refractories, A Comprehensive Handbook*, World Scientific Publishing, Singapore, 1998.
- [3] M.F. Zawrah, N.M. Khalil, Effect of Mullite Formation on Properties of Refractory Castables, *Ceramics International* 27/6 (2001) 689-694.
- [4] D.R. Dinger, J.E. Funk, Particle Packing II-Review of Packing of Polydisperse Particle Systems, *Interceram* 41/2 (1992) 95-97.
- [5] D.R. Dinger, J.E. Funk, Particle Packing III-Discrete Versus Continuous Particle Sizes, *Interceram* 41/5 (1992) 332-334.
- [6] A. Nishikawa, *Technology of Monolithic Refractories*, Plibrico Japan Company Limited, 1984.
- [7] A.F. Cardoso, M.D. Innocentini, M.A. Akiyoshi, V.C. Pandolfelli, Effect of Curing Condition on the Properties of Ultra-Low Cement Refractory Castables, *Refractories Applications and News* 9/2 (2004) 12-16.
- [8] A.F. Cardoso, M.D. Innocentini, M.A. Akiyoshi, V.C. Pandolfelli, Effect of Curing Time on the Properties of CAC Bonded Refractory Castables, *Journal of European Ceramic Society* 24 (2004) 2073-2078.